Phase-coherent electron transport in asymmetric crosslike Andreev interferometers

Pavel E. Dolgirev [1], Mikhail S. Kalenkov [2], Andrei E. Tarkhov [3], and Andrei D. Zaikin[4,5]

[1]*Department of Physics, Harvard University, Cambridge, Massachusetts 02138, USA*
[2]*I.E. Tamm Department of Theoretical Physics, P.N. Lebedev Physical Institute, 119991 Moscow, Russia*
[3]*Skolkovo Institute of Science and Technology, Skolkovo Innovation Center, 3 Nobel St., 143026 Moscow, Russia*
[4]*Institut für Nanotechnologie, Karlsruher Institut für Technologie (KIT), 76021 Karlsruhe, Germany*
[5]*National Research University Higher School of Economics, 101000 Moscow, Russia*

We present a detailed theoretical description of quantum coherent electron transport in voltage-biased crosslike Andreev interferometers. Making use of the charge conjugation symmetry encoded in the quasiclassical formalism, we elucidate a crucial role played by geometric and electron-hole asymmetries in these structures. We argue that a nonvanishing Aharonov-Bohm-like contribution to the current I_S flowing in the superconducting contour may develop only in geometrically asymmetric interferometers making their behavior qualitatively different from that of symmetric devices. The current I_N in the normal contour—along with I_S—is found to be sensitive to phase-coherent effects thereby also acquiring a 2π-periodic dependence on the Josephson phase. In asymmetric structures this current develops an odd-in-phase contribution originating from electron-hole asymmetry. We demonstrate that both phase-dependent currents I_S and I_N can be controlled and manipulated by tuning the applied voltage, temperature, and system topology, thus rendering Andreev interferometers particularly important for future applications in modern electronics.

I. INTRODUCTION

An interplay between quantum coherence and nonequilibrium phenomena is an intriguing topic in condensed matter physics. Hybrid metallic heterostructures composed of superconducting (S) and normal (N) terminals constitute an important playground to realize and investigate rich physics associated with the above phenomena. In these systems, frequently called Andreev interferometers, long-range quantum coherence is induced due to the superconducting proximity effect, while nonequilibrium conditions can be created by virtue of biasing different terminals with external voltages and/or temperature gradients [1–3]. Distinctive electrical and thermal properties of such systems, including, e.g., large phase-dependent thermoelectric effects [4–8], phase-coherent charge transport [9–15] and conductance reentrance [16,17], Aharonov-Bohm-like behavior of SN-rings [16–20] and nonlocal (or crossed) Andreev reflection [21–29], render them a promising platform for modern electronics and caloritronics.

Yet another remarkable effect is the so-called π-junction state that can occur in systems with two normal and two superconducting terminals interconnected by normal metallic wires forming a cross. Applying a phase twist ϕ to two superconducting terminals of this crosslike Andreev interferometer one induces dc Josephson current $I_S(\phi)$ between these terminals just like in usual SNS junctions [30–32]. Simultaneously biasing two normal terminals with an external voltage V one can modify the electron distribution function in the system, and thereby control the magnitude of $I_S \equiv I_S(\phi, V)$. At some values of V the supercurrent flowing between S terminals becomes negative signaling the π-junction state [33–36].

Recently three of us demonstrated [37,38] that the above scenario, being appropriate for symmetric crosslike Andreev interferometers, becomes by far incomplete as soon as the system topology is made asymmetric. It turns out that in the latter situation the underlying physics becomes much richer being essentially determined by a competition between voltage-dependent (odd in ϕ) Josephson and (even in ϕ) Aharonov-Bohm-like currents flowing in the superconducting contour. This tradeoff may have a drastic impact on the current-phase relation $I_S(\phi)$ in voltage-biased Andreev interferometers resulting in a novel (I_0, ϕ_0)-junction state [37], predicted to occur at low T and high enough eV exceeding an effective Thouless energy of our device. This state is characterized by coherent 2π-periodic oscillations of I_S as a function of ϕ shifted from the origin by the phase $\phi_0(V)$ that can take any value, thus being in general different from zero or π.

It should be emphasized that asymmetric topology of crosslike Andreev interferometers plays a crucial role for this effect: With the aid of simple charge-conjugation symmetry arguments to be outlined below one can demonstrate that by making the interferometer in Fig. 1 symmetric in at least one of the two contours (either normal or superconducting) one totally suppresses the Aharonov-Bohm contribution to I_S, hence, getting back to the physical picture [33–36] with $\phi_0(V) = 0, \pi$.

Here we will argue that the physics of asymmetric crosslike interferometers is actually even richer than that discussed in our previous studies [37,38]. In particular, it turns out that the current I_N flowing between the two normal terminals of such interferometer, similarly to I_S, exhibits proximity induced coherent 2π-periodic oscillations as a function of the superconducting phase difference ϕ. The function $I_N(\phi)$ is in
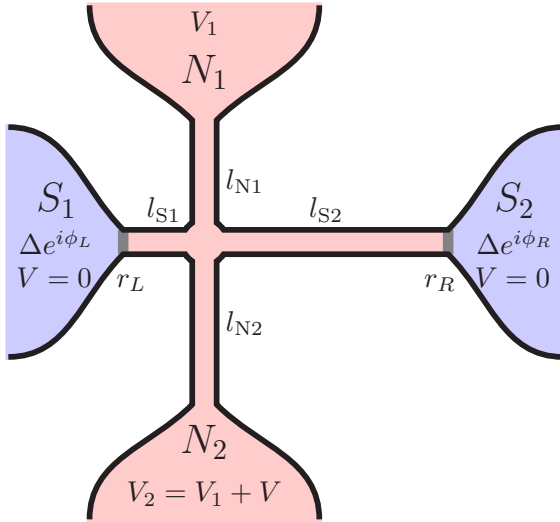
FIG. 1. Asymmetric crosslike Andreev interferometer under consideration.

general neither even nor odd, i.e., it consists of both even and odd in ϕ harmonics. While the first of these contributions ($\propto \cos\phi$) to the current I_N can be interpreted in terms of the Aharonov-Bohm-like effect, the second one ($\propto \sin\phi$) is much more tricky as it obviously cannot have anything to do with the Josephson current. Below we will demonstrate that the physical origin of the latter contribution to I_N is directly related to electron-hole asymmetry generated due to the mechanism of sequential Andreev reflections at different NS interfaces [39].

The structure of the paper is as follows. In Sec. II, we introduce the system under consideration, describe the quasiclassical formalism used throughout our paper, and elucidate the charge-conjugation symmetry properties of this formalism important for our further considerations. In Sec. III we focus our analysis on the limit of highly resistive NS interfaces, in which case it is possible to obtain a full analytic solution of our problem. Our key results and the corresponding discussion are formulated in Sec. IV. In Sec. V, we briefly summarize our findings. Further technical details are relegated to the Appendixes.

II. MODEL AND BASIC FORMALISM

Below we will consider crosslike Andreev interferometers schematically depicted in Fig. 1. The system consists of two normal-metal diffusive wires of total lengths $l_{N1} + l_{N2}$ and $l_{S1} + l_{S2} = L$ connected between each other in the form of a cross, and attached, respectively, to two normal and two superconducting terminals. We will address a general case of asymmetric Andreev interferometers with $l_{N1} \neq l_{N2}$ and $l_{S1} \neq l_{S2}$, which demonstrate a variety of quantum coherent effects some of which do not occur in symmetric configurations. Electrostatic potentials of both S terminals are set equal to zero $V = 0$, while the potentials of the normal terminals are denoted as V_1 and V_2. These N terminals are biased by an external voltage V implying $V_2 = V_1 + V$. The superconducting order parameter of the left and right S terminals is chosen

to be, respectively, $\Delta \exp(i\phi_L)$ and $\Delta \exp(i\phi_R)$. The value of the phase difference between these terminals $\phi = \phi_L - \phi_R$ can easily be controlled by an external magnetic flux inserted inside a superconducting loop.

Obviously, electric current can flow between S terminals (superconducting contour) as well as between N terminals (normal contour) being dependent on external bias V, temperature T, and phase difference ϕ. The task at hand is to determine the distribution of voltages and electric currents in our structure in the presence of long-range quantum coherent effects, and to demonstrate the importance of geometric and electron-hole asymmetries in our problem.

A. Quasiclassical formalism

We will adopt the standard quasiclassical formalism [1] aimed at describing nonequilibrium quantum properties of hybrid metallic structures like the one in Fig. 1. The quasiclassical Green's functions in each metallic wire are represented with the aid of a 4×4 matrices in the Keldysh-Nambu space composed of retarded ($\hat{G}^R$), advanced ($\hat{G}^A$), and Keldysh ($\hat{G}^K$) functions

$$\check{G}(\epsilon, \boldsymbol{r}) = \begin{pmatrix} \hat{G}^R & \hat{G}^K \\ \hat{0} & \hat{G}^A \end{pmatrix}. \tag{1}$$

This matrix Green's function obeys the normalization condition $\check{G}^2 = \check{I}$ and satisfies the Usadel equation

$$D\nabla(\check{G}\nabla\check{G}) = [-i\epsilon\hat{\tau}_z, \check{G}], \tag{2}$$

where D stands for a diffusion coefficient and $\hat{\tau}_z$ is the Pauli matrix in the Nambu space.

In what follows it will be convenient for us to employ the so-called Riccati parametrization [40,41]. For the retarded Green's function it reads

$$\hat{G}^R = \frac{1}{1 + \gamma\tilde{\gamma}} \begin{pmatrix} 1 - \gamma\tilde{\gamma} & 2\gamma \\ 2\tilde{\gamma} & \gamma\tilde{\gamma} - 1 \end{pmatrix}. \tag{3}$$

A similar representation holds for the advanced Green's function since $\hat{G}^A = -\hat{\tau}_z(\hat{G}^R)^+\hat{\tau}_z$. The spectral part of the Usadel equation then becomes

$$\Delta\gamma - \frac{2\tilde{\gamma}}{1 + \gamma\tilde{\gamma}}(\nabla\gamma)^2 + 2i\epsilon\gamma = 0, \tag{4}$$

$$\Delta\tilde{\gamma} - \frac{2\gamma}{1 + \gamma\tilde{\gamma}}(\nabla\tilde{\gamma})^2 + 2i\epsilon\tilde{\gamma} = 0. \tag{5}$$

With the aid of the standard representation for the Keldysh Green's function

$$\hat{G}^K = \hat{G}^R\hat{F} - \hat{F}\hat{G}^A, \quad \hat{F} = f_L + \hat{\tau}_z f_T, \tag{6}$$

the kinetic part of the Usadel equation can be cast to the form

$$\nabla j_L = 0, \quad j_L = D_L\nabla f_L - \mathcal{Y}\nabla f_T + j_s f_T, \tag{7}$$

$$\nabla j_T = 0, \quad j_T = D_T\nabla f_T + \mathcal{Y}\nabla f_L + j_s f_L. \tag{8}$$

Here $j_T = \mathrm{tr}(\check{G}\nabla\check{G}\hat{\tau}_z)^K$ and $j_L = \mathrm{tr}(\check{G}\nabla\check{G})^K$ represent the spectral densities of respectively electric and thermal currents, f_L and f_T are, respectively, symmetric and anisymmetric parts of the electron distribution function,

$$j_s = \frac{1}{4}\,\mathrm{tr}\,\hat{\tau}_z(\hat{G}^R\nabla\hat{G}^R - \hat{G}^A\nabla\hat{G}^A) \tag{9}$$

stands for the supercurrent density, and the kinetic coefficients D_L, D_T, and $\mathcal{Y}$ are defined as

$$D_L = \tfrac{1}{2} - \tfrac{1}{4} \operatorname{tr} \hat{G}^R \hat{G}^A, \tag{10}$$

$$D_T = \tfrac{1}{2} - \tfrac{1}{4} \operatorname{tr} \hat{G}^R \hat{\tau}_z \hat{G}^A \hat{\tau}_z, \tag{11}$$

$$\mathcal{Y} = \tfrac{1}{4} \operatorname{tr} \hat{G}^R \hat{\tau}_z \hat{G}^A. \tag{12}$$

Note that the kinetic coefficient (12) explicitly accounts for the presence of the electron-hole asymmetry in our system.

Resolving the Usadel equations one can evaluate the electric current density j in our system defined as

$$j = -\frac{\sigma_N}{2e} \int j_T(\epsilon)\, d\epsilon, \tag{13}$$

where σ_N is the Drude conductivity of a normal metal.

B. Boundary conditions

As usual, the Usadel equation (2) should be supplemented by proper boundary conditions allowing us to match the Green's functions at all intermetallic interfaces. Below we will assume that the central node—the contact between the two normal wires—is characterized by perfect transmission, meaning that the Green's functions are continuous and that the spectral currents associated with them are conserved. The same applies to the boundaries with the N terminals: The Green's functions inside the normal-metal wire are continuously matched to the corresponding bulk values $\hat{G}_N^{R/A} = \pm\hat{\tau}_z$ and

$$f_{L/T}^N = \frac{1}{2}\left[\tanh\frac{\epsilon + eV}{2T} \pm \tanh\frac{\epsilon - eV}{2T}\right]. \tag{14}$$

What remains is to define the boundary conditions at two NS interfaces. Here, we will restrict our analysis to the tunneling limit, i.e., we assume that the transmission of both NS interfaces is small compared to unity. This limit is accounted for by the well-known Kupriyanov-Lukichev (KL) boundary conditions [42]

$$L\check{G}\partial_x\check{G} = \pm\frac{1}{2r}[\check{G}_{\rm SC}, \check{G}], \tag{15}$$

where $\check{G}$ is the Green's function in the normal wire, $\check{G}_{\rm SC}$ denotes the bulk Green's function of the corresponding S terminal with

$$\hat{G}_{\rm SC}^R = \frac{\begin{pmatrix} \epsilon & \Delta e^{i\chi} \\ -\Delta e^{-i\chi} & -\epsilon \end{pmatrix}}{\sqrt{(\epsilon + i\delta)^2 - \Delta^2}}, \tag{16}$$

$$\hat{G}_{\rm SC}^K = \tanh\frac{\epsilon}{2T}(\hat{G}_{\rm SC}^R - \hat{G}_{\rm SC}^A), \tag{17}$$

and phase χ equals to either ϕ_L or ϕ_R depending on the terminal. The parameter r is defined as

$$r = \frac{\mathcal{A}\sigma_N}{L\mathcal{G}}, \tag{18}$$

where $\mathcal{A}$ is the interface cross section and $\mathcal{G}$ is the normal-state conductance of the interface. Note that within the applicability range of KL boundary conditions (15) and depending on the relation between $\mathcal{G}$ and the conductance of the normal wire of

length L, the parameter r can in general take any value both smaller and larger than unity.

C. Symmetry considerations

Let us define charge-conjugated Green's function as

$$\check{G}_c(\epsilon, \boldsymbol{r}) = -\hat{\tau}_1 \check{G}(\epsilon, \boldsymbol{r})\hat{\tau}_1. \tag{19}$$

It is straightforward to verify that the function (19) represents a solution of the Usadel equation (2) with inverted signs of both electric and magnetic fields as well as of that of the superconducting phase. This symmetry has important consequences for the charge transport properties of the system under consideration.

Resolving the Usadel equation (2) we determine the charge currents in all four metallic wires as functions of the phase difference ϕ and the applied voltages V_1 and V_2. Making use of Eq. (19) one can demonstrate that all currents invert their signs under the transformation $V_1 \leftrightarrow -V_1$, $V_2 \leftrightarrow -V_2$, $\phi \leftrightarrow -\phi$, i.e., we have

$$I_i(-\phi, -V_1, -V_2) = -I_i(\phi, V_1, V_2), \tag{20}$$

where the index i labels the wires $N1$, $N2$, $S1$, and $S2$.

The electrostatic potentials V_1 and V_2 as functions of both the phase ϕ and the bias voltage V are determined from the current conservation conditions

$$I_{N1}(\phi, V_1, V_2) = I_{N2}(\phi, V_1, V_2) = I_N, \tag{21}$$

$$I_{S1}(\phi, V_1, V_2) = I_{S2}(\phi, V_1, V_2) = I_S, \tag{22}$$

combined with the condition $V_2 - V_1 = V$. Likewise, the currents I_{S1}, I_{S2}, I_{N1}, I_{N2} can also be expressed as functions of ϕ and V.

In general all these currents are 2π-periodic functions of ϕ. Extra geometric symmetries of our structure may enforce higher symmetries for the above currents rendering them, e.g., either purely even or purely odd functions of ϕ. In particular, it is instructive to distinguish two special cases: (i) symmetric connectors to S terminals (implying that $l_{S1} = l_{S2}$ and $r_L = r_R$) and (ii) symmetric connectors to N terminals ($l_{N1} = l_{N2}$). It follows immediately (see also Appendix A for more details) that in both cases (i) and (ii) the current I_S turns out to be an odd function of ϕ, i.e.,

$$I_S(-\phi) = -I_S(\phi), \tag{23}$$

whereas the current I_N is even in ϕ,

$$I_N(-\phi) = I_N(\phi). \tag{24}$$

Hence, for partially symmetric crosslike Andreev interferometers [in both cases (i) and (ii)] the Aharonov-Bohm-like contribution to the current I_S vanishes and we are back to the situation of only 0- or π-junction states considered in Refs. [33–35]. On top of that, no odd-in-ϕ contribution to I_N can occur in such structures. In what follows we will, therefore, address the most general case of fully asymmetric interferometers with $l_{N1} \neq l_{N2}$ and $l_{S1} \neq l_{S2}$.

III. HIGHLY RESISTIVE INTERFACES: ANALYTIC SOLUTION

Let us now employ the above equations and evaluate the Green's functions for the structure depicted in Fig. 1. As usual, one can split the problem into spectral, Eqs. (4)–(5), and kinetic, Eqs. (7)–(8), parts, which can be treated separately. Below in this section, we will stick to the limit of sufficiently large values of the parameter r at both NS interfaces and construct a full analytic solution of the problem.

A. Spectral part

Let us assume that tunnel barriers at both NS interfaces are sufficiently large and, hence, anomalous correlations penetrating into the normal-metal wires from the superconducting terminals are strongly suppressed. In this case, one can linearize the spectral part of the Usadel equation and get

$$\gamma_i'' + \lambda^2 \gamma_i = 0, \tag{25}$$

where $\lambda^2 = 2i\epsilon/(\mathcal{E}_{\text{Th}}L^2)$ and $\mathcal{E}_{\text{Th}} \equiv D/L^2$ (with $L = l_{\text{S1}} + l_{\text{S2}}$) is an effective Thouless energy of our setup. The same equation also holds for $\tilde{\gamma}$. Here and below, we also assume $\mathcal{E}_{\text{Th}} \ll \Delta$ enabling us to restrict our analysis to subgap energies $|\epsilon| < \Delta$.

The boundary conditions take the form

$$\gamma_{\text{S1}}(0) = \gamma_{\text{S2}}(0) = \gamma_{\text{N1}}(0) = \gamma_{\text{N2}}(0) = \gamma_0,$$

$$\mathcal{A}_{\text{S1}}\gamma_{\text{S1}}'(0) + \mathcal{A}_{\text{N2}}\gamma_{\text{N2}}'(0) = \mathcal{A}_{\text{S2}}\gamma_{\text{S2}}'(0) + \mathcal{A}_{\text{N1}}\gamma_{\text{N1}}'(0),$$

$$\gamma_{\text{N1}}(l_{\text{N1}}) = \gamma_{\text{N2}}(-l_{\text{N2}}) = 0,$$

$$L\gamma_{\text{S1}}'(-l_{\text{S1}}) = -\frac{\mathcal{F}_L}{2r_L}, \quad L\gamma_{\text{S2}}'(l_{\text{S2}}) = \frac{\mathcal{F}_R}{2r_R}.$$

Equations in the first two lines follow directly from the continuity of γ and from the spectral current conservation at the central node (with coordinate set equal to zero). The equation in the third line implies that anomalous correlations vanish at the boundaries with both N terminals. Finally, the two equations in the last line just represent KL boundary conditions at the left and right NS interfaces characterized by parameters r_L and r_R, respectively, [defined in Eq. (18) with $\mathcal{G} \equiv \mathcal{G}_{L/R}$]. We also choose

$$\mathcal{F}_R = \frac{-i\Delta e^{i\phi_R}}{\sqrt{\Delta^2 - (\epsilon + i\delta)^2}}, \quad \mathcal{F}_L = \frac{-i\Delta e^{i\phi_L}}{\sqrt{\Delta^2 - (\epsilon + i\delta)^2}}.$$

Resolving the linearized Usadel equations with the above boundary conditions, we obtain

$$\gamma_{\text{N1}} = \gamma_0 \frac{\sin \lambda(l_{\text{N1}} - x)}{\sin \lambda l_{\text{N1}}}, \quad \gamma_{\text{N2}} = \gamma_0 \frac{\sin \lambda(l_{\text{N2}} + x)}{\sin \lambda l_{\text{N2}}}, \tag{26}$$

$$\gamma_{\text{S1}} = \gamma_0 \frac{\cos \lambda(l_{\text{S1}} + x)}{\cos \lambda l_{\text{S1}}} - \frac{\mathcal{F}_L}{2L\lambda r_L} \frac{\sin \lambda x}{\cos \lambda l_{\text{S1}}}, \tag{27}$$

$$\gamma_{\text{S2}} = \gamma_0 \frac{\cos \lambda(l_{\text{S2}} - x)}{\cos \lambda l_{\text{S2}}} + \frac{\mathcal{F}_R}{2L\lambda r_R} \frac{\sin \lambda x}{\cos \lambda l_{\text{S2}}}, \tag{28}$$

where

$$\gamma_0 = \frac{1}{\mathcal{N}} \frac{1}{2L\lambda} \left(\frac{\mathcal{F}_L \mathcal{A}_{\text{S1}}}{r_L \cos \lambda l_{\text{S1}}} + \frac{\mathcal{F}_R \mathcal{A}_{\text{S2}}}{r_R \cos \lambda l_{\text{S2}}} \right), \tag{29}$$

$$\mathcal{N} = \mathcal{A}_{\text{N1}} \cot \lambda l_{\text{N1}} + \mathcal{A}_{\text{N2}} \cot \lambda l_{\text{N2}} -$$
$$- \mathcal{A}_{\text{S1}} \tan \lambda l_{\text{S1}} - \mathcal{A}_{\text{S2}} \tan \lambda l_{\text{S2}}. \tag{30}$$

Then, for the spectral supercurrent density, one readily finds

$$j_{s,\text{S1}} \mathcal{A}_{\text{S1}} = j_{s,\text{S2}} \mathcal{A}_{\text{S2}} = \frac{\mathcal{A}_{\text{S1}} \mathcal{A}_{\text{S2}}}{L^2 r_R r_L} \sin \phi$$

$$\times \text{Re} \left\{ \frac{\Delta^2}{\Delta^2 - (\epsilon + i\delta)^2} \frac{i}{\lambda \cos \lambda l_{\text{S1}} \cos \lambda l_{\text{S2}}} \frac{1}{\mathcal{N}} \right\}. \tag{31}$$

The above analytic solution of the spectral part of the problem enables one to easily derive the applicability condition for the linearized Usadel equation (25). Setting functions γ to be much smaller than unity within the normal wires and making use of Eqs. (26)–(30), we arrive at the following conditions:

$$r_L \gg \frac{\mathcal{A}_{\text{S1}}}{L \left(\frac{\mathcal{A}_{\text{N1}}}{l_{\text{N1}}} + \frac{\mathcal{A}_{\text{N2}}}{l_{\text{N2}}} \right)}, \quad r_R \gg \frac{\mathcal{A}_{\text{S2}}}{L \left(\frac{\mathcal{A}_{\text{N1}}}{l_{\text{N1}}} + \frac{\mathcal{A}_{\text{N2}}}{l_{\text{N2}}} \right)}. \tag{32}$$

Note that depending on the system parameters these conditions may substantially deviate from simple inequalities $r_{R,L} \gg 1$, which one could naively expect to be sufficient in order to linearize the Usadel equations.

B. Kinetic part

Below, we proceed similarly to the above Sec. III A, and resolve the kinetic equations perturbatively by formally expanding them in $1/(r_i r_j)$, where $i, j = L, R$. In the zeroth order, we have

$$\nabla j_{L/T}^{(0)} = 0, \quad j_{L/T}^{(0)} = \nabla f_{L/T}^{(0)} \tag{33}$$

with the boundary conditions

$$f_{L/T}^{(0)}(l_{\text{N1}}, \epsilon) = f_{L/T}^N(V_1), \quad f_{L/T}^{(0)}(-l_{\text{N2}}, \epsilon) = f_{L/T}^N(V_2);$$

$$j_{L,\text{S1/S2}}^{(0)} = j_{T,\text{S1/S2}}^{(0)} = 0;$$

$$\mathcal{A}_{\text{S1}} j_{L/T,\text{S1}} + \mathcal{A}_{\text{N2}} j_{L/T,\text{N2}} = \mathcal{A}_{\text{S2}} j_{L/T,\text{S2}} + \mathcal{A}_{\text{N1}} j_{L/T,\text{N1}}.$$

Equations in the first line account for boundaries with both N terminals, the second line represents KL boundary conditions at both NS interfaces, whereas the last equation just reflects both electric and energy currents conservation and, hence, it remains valid to all orders. In fact, the condition $j_{L,\text{S1/S2}} = 0$ is also valid to all orders at energies $|\epsilon| < \Delta$, since subgap excitations do not contribute to the energy current flowing into the S terminals.

We observe that—to the zeroth order—functions $f_L^{(0)}$ and $f_T^{(0)}$ depend linearly on the coordinate along the wire in the normal contour, whereas in the wire that belongs to the superconducting contour these functions remain constant equal to

$$f_{L/T}^{(0)}(0) = \left(\frac{1}{R_{\text{N1}}} + \frac{1}{R_{\text{N2}}} \right)^{-1} \left[\frac{f_{L/T}^N(V_1)}{R_{\text{N1}}} + \frac{f_{L/T}^N(V_2)}{R_{\text{N2}}} \right]. \tag{34}$$

Here, R_{N1} and R_{N2} are normal-state Drude resistances of the normal wires connected to terminals N_1 and N_2

$$R_{N1} = \frac{l_{N1}}{\mathcal{A}_{N1}\sigma_N}, \quad R_{N2} = \frac{l_{N2}}{\mathcal{A}_{N2}\sigma_N}. \tag{35}$$

Note that with the aid of the above zeroth-order solution combined with KL boundary conditions one can establish the spectral electric current in the superconducting contour to the next order in parameter $\sim 1/(r_L r_R)$. Indeed, the latter conditions can be written in the form $j_T^{(1)} = \pm \alpha_T/(L r_{L/R})$

with

$$\alpha_T = \mathrm{Im}\left\{\frac{\Delta(e^{-i\phi}\gamma + e^{i\phi}\tilde{\gamma})}{\sqrt{\Delta^2 - (\epsilon + i\delta)^2}}\right\} f_L^{(0)}$$
$$- \mathrm{Im}\left\{\frac{\Delta(e^{-i\phi}\gamma - e^{i\phi}\tilde{\gamma})}{\sqrt{\Delta^2 - (\epsilon + i\delta)^2}}\right\} f_T^{(0)}. \tag{36}$$

With this in mind, the electric current conservation condition yields

$$\mathcal{A}_{S1}\int d\epsilon\, j_{T,S1}(\epsilon) = \mathcal{A}_{S2}\int d\epsilon\, j_{T,S2}(\epsilon), \tag{37}$$

which after some algebra can further be cast to the form

$$\frac{\mathcal{A}_{S2}}{r_R^2}\int d\epsilon f_T^{(0)}\,\mathrm{Im}\left\{\frac{\Delta^2}{\Delta^2 - (\epsilon + i\delta)^2}\frac{i}{\lambda}\frac{\tan\lambda l_{S2}(\mathcal{A}_{N1}\cot\lambda l_{N1} + \mathcal{A}_{N2}\cot\lambda l_{N2} - \mathcal{A}_{S1}\tan\lambda l_{S1}) + \mathcal{A}_{S2}}{\mathcal{N}}\right\}$$
$$+ 2\frac{\mathcal{A}_{S1}\mathcal{A}_{S2}}{r_R r_L}\cos\phi\int d\epsilon f_T^{(0)}\,\mathrm{Im}\left\{\frac{\Delta^2}{\Delta^2 - (\epsilon + i\delta)^2}\frac{i}{\lambda\cos\lambda l_{S1}\cos\lambda l_{S2}}\frac{1}{\mathcal{N}}\right\}$$
$$+ \frac{\mathcal{A}_{S1}}{r_L^2}\int d\epsilon f_T^{(0)}\,\mathrm{Im}\left\{\frac{\Delta^2}{\Delta^2 - (\epsilon + i\delta)^2}\frac{i}{\lambda}\frac{\tan\lambda l_{S1}(\mathcal{A}_{N1}\cot\lambda l_{N1} + \mathcal{A}_{N2}\cot\lambda l_{N2} - \mathcal{A}_{S2}\tan\lambda l_{S2}) + \mathcal{A}_{S1}}{\mathcal{N}}\right\} = 0. \tag{38}$$

This equation together with the condition $V_2 - V_1 = V$ defines electrostatic potentials of both normal terminals V_1 and V_2 demonstrating that these potentials depend not only on V and T, but also on phase difference ϕ between the superconducting terminals. The latter dependence clearly illustrates the importance of long-range proximity induced quantum coherence effects spreading not only into the superconducting contour but also into the normal contour, thereby influencing the potentials of both normal terminals. It follows from Eq. (38) that both electrostatic potentials V_1 and V_2 depend on $\cos\phi$, thus being even functions of ϕ.

The above perturbative analysis of the kinetic equations can be justified if the interface resistances are much larger than the resistances of the corresponding attached normal wires

$$r_L L/l_{S1}, \; r_R L/l_{S2} \gg 1. \tag{39}$$

Having determined V_1 and V_2, we are ready to find the electric current in the superconducting contour. It reads

$$I_S = -\frac{\sigma_N}{2e}\int d\epsilon\,\mathcal{A}_{S1}\,j_{T,S1}(\epsilon), \tag{40}$$

where

$$\mathcal{A}_{S1}j_{T,S1} = f_L^{(0)}\frac{\mathcal{A}_{S1}\mathcal{A}_{S2}}{L^2 r_R r_L}\sin\phi\,\mathrm{Re}\left\{\frac{\Delta^2}{\Delta^2 - (\epsilon + i\delta)^2}\frac{i}{\lambda\cos\lambda l_{S1}\cos\lambda l_{S2}}\frac{1}{\mathcal{N}}\right\}$$
$$+ f_T^{(0)}\frac{\mathcal{A}_{S1}\mathcal{A}_{S2}}{L^2 r_R r_L}\cos\phi\,\mathrm{Im}\left\{\frac{\Delta^2}{\Delta^2 - (\epsilon + i\delta)^2}\frac{i}{\lambda\cos\lambda l_{S1}\cos\lambda l_{S2}}\frac{1}{\mathcal{N}}\right\}$$
$$+ f_T^{(0)}\frac{\mathcal{A}_{S1}}{L^2 r_L^2}\,\mathrm{Im}\left\{\frac{\Delta^2}{\Delta^2 - (\epsilon + i\delta)^2}\frac{i}{\lambda}\frac{\tan\lambda l_{S1}(\mathcal{A}_{N1}\cot\lambda l_{N1} + \mathcal{A}_{N2}\cot\lambda l_{N2} - \mathcal{A}_{S2}\tan\lambda l_{S2}) + \mathcal{A}_{S1}}{\mathcal{N}}\right\}. \tag{41}$$

The first term in the right-hand side of Eq. (41) represents the Josephson contribution, the second term [proportional to both $1/(r_L r_R)$ and $\cos\phi$] defines the coherent Aharonov-Bohm-like current, while the last term has to do with the Andreev conductance of SN interfaces.

As already mentioned above, Eq. (38) contains only terms depending on $\cos\phi$, while the Josephson contribution proportional to $\sin\phi$ drops out from this equation. In other words, the terms entering the electric current conservation condition, cf. Eq. (37), represent the combination of $\cos\phi$-dependent (Aharonov-Bohm) and ϕ-independent (Andreev) contributions. This observation appears to be specific to the chosen crosslike geometry [as suggested, e.g., by Eqs. (31) and (34)] and, furthermore, it only holds in the leading order

in $1/(r_i r_j)$. A more detailed numerical analysis indicates that for smaller values of $r_{L,R}$ the $\sin\phi$ harmonic is present and might even play an important role. We also note that Eq. (38) and Eq. (41) can be combined in a way that allows us to expel an explicit dependence on $\cos\phi$ from the expression for I_S. In this case, the even in ϕ contribution to I_S appears implicitly due to the dependencies of potentials V_1 and V_2 on ϕ.

IV. RESULTS AND DISCUSSION

Let us now explicitly evaluate the distribution of voltages and currents in our crosslike Andreev interferometer. We first determine electrostatic potentials of the two normal
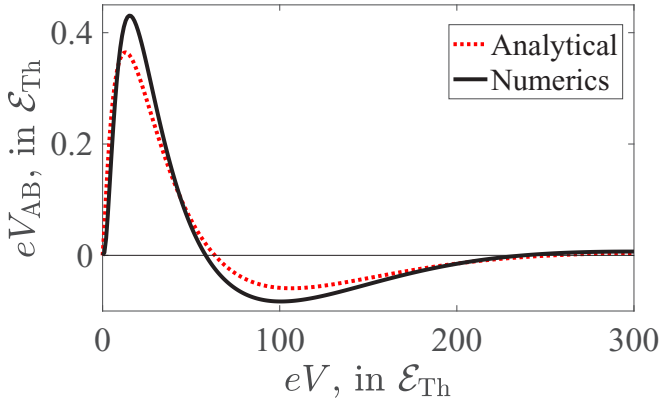
FIG. 2. The amplitude of even-in-ϕ oscillations of electrostatic potentials $V_{1/2}$ as a function of the bias voltage V at $T \mapsto 0$. Numerical curve (solid line) is obtained by solving Eq. (38). An approximate result (44) is indicated by the dotted red line. Here we set $r_L = r_R = r \gg 1$, $l_{S1} \equiv L - l_{S2} = 0.2L$, $l_{N1} = 0.3L$, $l_{N2} = 0.7L$, and $\Delta = 500\mathcal{E}_{\text{Th}}$. Note that this amplitude does not depend on r in the limit of large r.

terminals, V_1 and V_2, and then evaluate the currents in both superconducting and normal contours, which depend on these potentials.

A. Electrostatic potentials

According to Eq. (38) the corresponding Aharonov-Bohm term is proportional to $\sim 1/(r_L r_R)$, i.e., it has the same order as the other two terms $\sim 1/r_L^2$ and $\sim 1/r_R^2$. On the other hand, in the limit $l_{S1}, l_{S2} \gg \sqrt{D/\Delta}$ considered here and at high enough voltages $\mathcal{E}_{\text{Th}} \ll e|V_{1,2}| < |\Delta|$ the Aharonov-Bohm contribution becomes exponentially suppressed as $\propto e^{-\sqrt{e|V_{1,2}|/\mathcal{E}_{\text{Th}}}}$ and, hence, it can be treated as a small perturbation. Then we obtain

$$V_{1/2} \approx \bar{V}_{1/2}(V) + V_{\text{AB}}(V)\cos\phi, \quad (42)$$

where

$$\bar{V}_1 \approx -\frac{R_{N1}^2}{R_{N1}^2 + R_{N1}^2}V, \quad \bar{V}_2 \approx \frac{R_{N2}^2}{R_{N1}^2 + R_{N1}^2}V \quad (43)$$

and

$$eV_{\text{AB}} = \frac{4r_R r_L}{r_R^2 + r_L^2}\frac{(R_{N1}R_{N2})^2}{(R_{N1}^2 + R_{N2}^2)^{3/2}}\sqrt{e|V|\mathcal{E}_{\text{Th}}}\left[\frac{e^{-\sqrt{e|\bar{V}_2|/\mathcal{E}_{\text{Th}}}}}{R_{N2}}\right.$$

$$\times \sin\sqrt{e|\bar{V}_2|/\mathcal{E}_{\text{Th}}} - \left.\frac{e^{-\sqrt{e|\bar{V}_1|/\mathcal{E}_{\text{Th}}}}}{R_{N1}}\sin\sqrt{e|\bar{V}_1|/\mathcal{E}_{\text{Th}}}\right]. \quad (44)$$

The presence of the ϕ-dependent term in Eq. (42) indicates that electrostatic potentials $V_{1/2}$ are sensitive to proximity-induced long-range quantum coherence in our structure. The magnitude of this coherent contribution to $V_{1,2}$ is controlled by parameter V_{AB} defined in Eq. (44). Note that this approximate analytic expression for V_{AB} turns out to be very accurate, as it is demonstrated in Fig. 2.

B. Current I_S in the superconducting contour

Following our previous analysis [37,38] we can express the current I_S in the superconducting contour in the form

$$I_S(\phi, V) = I_S^{\text{even}}(\phi, V) + I_S^{\text{odd}}(\phi, V)$$

$$\approx I_0(V) + I_J(V)\sin\phi + I_{\text{AB}}(V)\cos\phi. \quad (45)$$

Here $I_0(V)$ defines a dissipative Andreev-like term entering Eq. (41), while I_J and I_{AB} represent odd in ϕ Josephson and even in ϕ Aharonov-Bohm-like currents. It follows directly from Eq. (38) that the last (Aharonov-Bohm) term differs from zero only for asymmetric structures with both $l_{S1} \neq l_{S2}$ and $l_{N1} \neq l_{N2}$, in accordance with our general symmetry analysis in Sec. II C.

The results derived in the previous subsection imply that in the particular case of identical NS boundaries with $r_L = r_R = r \gg 1$ we have $I_S(r) \propto 1/r^2$. In this limit, the amplitudes of both odd and even in ϕ oscillations as functions of V are shown in Fig. 3. We observe that $I_J(V)$ experiences zero-to-π-junction switching [33–36] at around $eV \simeq 17\mathcal{E}_{\text{Th}}$ and becomes exponentially suppressed at higher voltages, similarly to the case of fully transparent NS boundaries [37,38]. Integrating the supercurrent density in Eq. (41) over energies, at sufficiently high bias voltages $eV \gg \mathcal{E}_{\text{Th}}$ we get

$$\frac{eR_L I_J}{\mathcal{E}_{\text{Th}}} \approx \frac{1}{r_R r_L}\sum_{i=1,2}\frac{1/R_{Ni}}{1/R_{N1} + 1/R_{N2}}\frac{\Delta^2}{\Delta^2 - (e\bar{V}_i)^2}$$

$$\times e^{-\sqrt{e|\bar{V}_i|/\mathcal{E}_{\text{Th}}}}\cos\sqrt{\frac{e|\bar{V}_i|}{\mathcal{E}_{\text{Th}}}}. \quad (46)$$

This formula turns out to be in a good agreement with the numerical solution of Eq. (38) at $eV \gtrsim 5\mathcal{E}_{\text{Th}}$, cf. Fig. 3(a).

Just like in the case of transparent SN boundaries [37,38], here one could expect $I_{\text{AB}}(r, V)$ to saturate to some nonzero value $I_{\text{AB}}^\infty(r)$ at sufficiently high voltages $eV \gg \mathcal{E}_{\text{Th}}$. In contrast to such expectations, in the limit $r \gg 1$ one finds $I_{\text{AB}}^\infty = 0$, cf. also Fig. 3(b). The latter result applies in the leading order in $1/r^2$ and has the same origin as a similar behavior of the coherent contribution to $V_{1/2}$ at large voltages, cf. Fig. 2. Hence, one can expect that $I_{\text{AB}}^\infty(r) \propto 1/r^4$ for $r \gg 1$.

For amplitude $I_{\text{AB}}(V)$, within the voltage interval $\Delta \gg eV \gg \mathcal{E}_{\text{Th}}$, one can derive an expression similar to the one in Eq. (46). Under the condition $l_{S1}, l_{S2} \gg \sqrt{D/(eV)}$ we obtain

$$\frac{eR_L I_{\text{AB}}}{\mathcal{E}_{\text{Th}}} \approx \frac{r_L^2 - r_R^2}{(r_L^2 + r_R^2)r_R r_L}\frac{R_{N1}R_{N2}}{R_{N1} + R_{N2}}$$

$$\times \sum_{i=1,2}\frac{(-1)^i}{R_{Ni}}e^{-\sqrt{e|\bar{V}_i|/\mathcal{E}_{\text{Th}}}}\sin\sqrt{\frac{e|\bar{V}_i|}{\mathcal{E}_{\text{Th}}}}. \quad (47)$$

Note that in the particular case $r_R = r_L = r$, the expression (47) vanishes identically implying that a more accurate treatment is required in this case. The corresponding analysis can

be worked out and yields

$$\frac{eR_L I_{AB}}{\mathcal{E}_{Th}} \approx -\frac{1}{2r^2} \frac{R_{N1}R_{N2}}{(R_{N1}+R_{N2})(R_{N1}^2+R_{N2}^2)} \left[\sum_{i=1,2} \frac{(-1)^i}{R_{Ni}} e^{-\sqrt{e|\bar{V}_i|/\mathcal{E}_{Th}}} \sin\sqrt{\frac{e|\bar{V}_i|}{\mathcal{E}_{Th}}} \right]$$

$$\times \left\{ \sum_{i,j=1,2} (-1)^j R_{Ni}^2 \exp\left(-\sqrt{\frac{e|\bar{V}_i|}{\mathcal{E}_{Th}}}\frac{l_{Sj}}{L}\right) \left[\cos\left(\sqrt{\frac{e|\bar{V}_i|}{\mathcal{E}_{Th}}}\frac{l_{Sj}}{L}\right) - \sin\left(\sqrt{\frac{e|\bar{V}_i|}{\mathcal{E}_{Th}}}\frac{l_{Sj}}{L}\right) \right] \right\}. \qquad (48)$$

As far as the temperature dependence of I_S is concerned, we point out that, while the Aharonov-Bohm-like contribution I_{AB} decays as a power law with increasing $T > eV$, the Josephson term I_J decays exponentially, thus becoming negligible as compared to I_{AB} in the high-temperature limit $T \gg \mathcal{E}_{Th}$. In the case of fully transparent NS interfaces the temperature dependencies of both even and odd in ϕ components of I_S have already been studied elsewhere [37,38], therefore we can avoid further details here.

C. Current I_N in the normal contour

Let us now turn to the electric current I_N flowing between the two normal terminals. This current also demonstrates a 2π-periodic dependence on phase ϕ and can be represented as a sum of even and odd in ϕ contributions:

$$I_N(\phi, V) = I_N^{even}(\phi, V) + I_N^{odd}(\phi, V). \qquad (49)$$

The first (even-in-ϕ) term again describes the Aharonov-Bohm-like contribution [43] and is by no means surprising. At the same time, the presence of the odd periodic in ϕ

contribution to current I_N is curious. In contrast to the superconducting contour, here term $I_N^{odd}(\phi, V)$ obviously cannot be attributed to the Josephson effect, and its physical nature requires further analysis.

For simplicity, let us assume that all cross sections are equal $\mathcal{A}_i = \mathcal{A}$. Then, we obtain

$$I_N^{odd} = \frac{\sigma_N}{2e} \frac{\mathcal{A}}{l_{N1}+l_{N2}} \int d\epsilon\, j_L^{(0)} \int_{-l_{N2}}^{l_{N1}} dx\, \mathcal{Y}(x,\epsilon), \qquad (50)$$

where $j_L^{(0)} = (f_L^N(V_1) - f_L^N(V_2))/(l_{N1}+l_{N2})$ is the corresponding spectral current in the normal contour. Since the current I_N^{odd} in Eq. (50) is controlled by the kinetic coefficient $\mathcal{Y}$ we conclude that this current should be attributed to the electron-hole asymmetry in our system generated due to the phase-sensitive mechanism of sequential Andreev reflections at different NS interfaces [39]. This conclusion is further supported by observing that $I_N^{odd} \propto \sin\phi/(r_L r_R)$.

At sufficiently large voltages $e|V| \gg \mathcal{E}_{Th}$ the integrals in Eq. (50) can be handled explicitly, and we get

$$\frac{eR_L I_N^{odd}}{\mathcal{E}_{Th}} \approx \frac{\sin\phi}{16 r_R r_L} \frac{(R_{S1}+R_{S2})^2}{(R_{N1}+R_{N2})^2} \frac{L^2}{l_{S1}^2+l_{S2}^2} \sum_{i=1,2} (-1)^{i+1} \frac{\mathcal{E}_{Th}}{e|\bar{V}_i|} \frac{\Delta^2}{\Delta^2 - (e\bar{V}_i)^2} e^{-\sqrt{e|\bar{V}_i|/\mathcal{E}_{Th}}}$$

$$\times \left[\sin\left(\sqrt{\frac{e|\bar{V}_i|}{\mathcal{E}_{Th}}}\frac{l_{S1}-l_{S2}}{L}\right) + \frac{l_{S1}-l_{S2}}{L}\cos\left(\sqrt{\frac{e|\bar{V}_i|}{\mathcal{E}_{Th}}}\frac{l_{S1}-l_{S2}}{L}\right) \right], \qquad (51)$$

where $R_{S1} = l_{S1}/(\mathcal{A}_{S1}\sigma_N)$ and $R_{S2} = l_{S2}/(\mathcal{A}_{S2}\sigma_N)$ are the normal state Drude resistances of the wires connected to the superconducting terminals. We also note that the current in Eq. (51) vanishes identically for $l_{S1} = l_{S2}$ (and $r_{S1} = r_{S2}$) and/or $l_{N1} = l_{N2}$, in full agreement with our symmetry considerations in Sec. II C.

It is also interesting to study current $I_N(\phi, V)$ at different values of r. This can be done by numerically solving the Usadel equation (2). In Fig. 4 we display the corresponding results for the amplitudes of both odd and even oscillations of the current I_N as functions of V at $T \mapsto 0$ for different values of r. We observe that the odd in ϕ harmonics persists at all values of r becoming progressively more pronounced with decreasing r, cf. also the inset in Fig. 4 where we present the result obtained in the limit $r = 0$. This amplitude first increases with increasing V reaching its maximum at around $eV \simeq 10\mathcal{E}_{Th}$ and then falls off being exponentially suppressed already at $eV \simeq 50\mathcal{E}_{Th}$ in accordance with Eq. (51). Let us

mention that in contrast to the current $I_J(V)$, which exhibits the transition to the π-junction state [37,38] at around $eV \gtrsim 15\mathcal{E}_{Th}$ [cf. also Fig 3(a)], the amplitude of $I_N^{odd}(V)$ demonstrates similar switching at much higher voltages $eV \gtrsim 60\mathcal{E}_{Th}$. This behavior of $I_N^{odd}(V)$ is related to the presence of an extra parameter $(l_{S1} - l_{S2})/L < 1$ in the argument of the sin term, cf. Eq. (51).

The even in ϕ current amplitude $I_N^{even}(V)$ saturates to a nonzero value at large voltages (see Fig. 4), just as one would expect for the Aharonov-Bohm-like contribution. Notably, the value of the plateau scales as $1/r^2$ for $r \gg 1$. This is in contrast to $I_{AB}^\infty(r)$, which scales as $1/r^4$.

In order to complete our analysis of the current I_N, we note that with increasing temperature $T > eV$ the even-in-ϕ contribution to this current decays as a power law similarly to $I_{AB}(T)$, which could serve as a signature of the Aharonov-Bohm-like effect. In contrast, the odd-in-ϕ contribution $I_N^{odd}(T)$ behaves qualitatively similarly to the
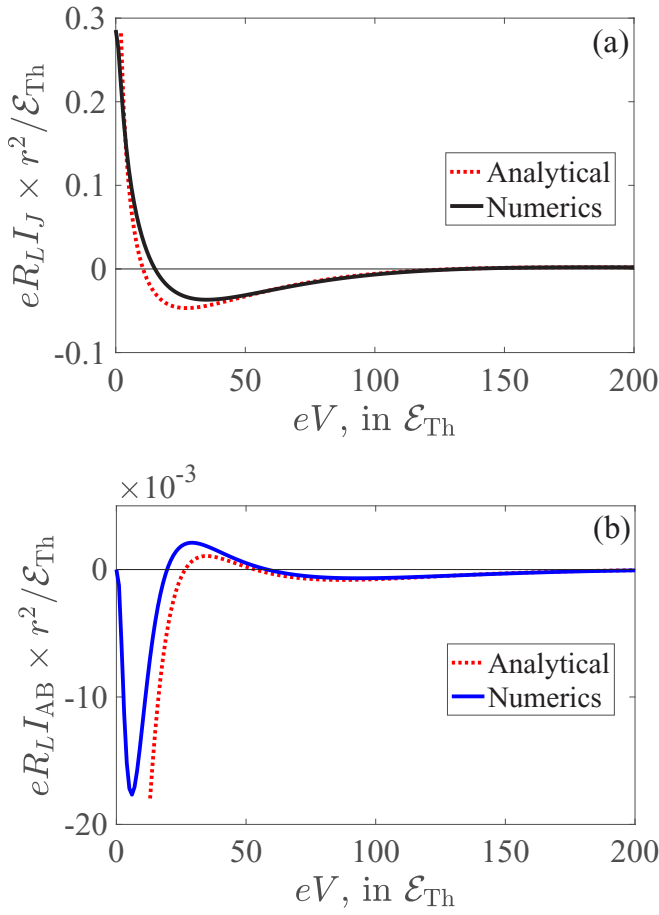
FIG. 3. The amplitudes of (a) odd-in-ϕ and (b) even-in-ϕ oscillations of the current I_S as functions of V at $T \mapsto 0$. Numerical curves (indicated by solid lines) are obtained by solving Eq. (38). Analytical results (dotted red lines) correspond to Eq. (46) in (a) and to Eq. (48) in (b).

Josephson term $I_J(T)$ decaying much faster than $I_N^{\text{even}}(T)$ and becoming invisibly small already at temperatures of order several $\mathcal{E}_{\text{Th}}$.

V. CONCLUSIONS

In this work we performed a detailed analysis of a nontrivial interplay between proximity induced long-range quantum coherence and nonequilibrium effects in crosslike Andreev interferometers as well as of its impact on electron transport properties of such devices.

We emphasized a crucial role of various symmetries in our problem. The charge conjugation symmetry encoded in the Usadel equations allowed us to establish an important general relation (20), which, in turn, helps to demonstrate that topology of crosslike Andreev interferometers is essential for determining charge transport properties of these devices.

We showed that in symmetric interferometers, the current I_S in the superconducting contour is an odd function of the superconducting phase difference ϕ. In other words, the even-in-ϕ Aharonov-Bohm-like contribution vanishes identically in such structures. These setups can only support the voltage-controlled Josephson current, and demonstrate switching
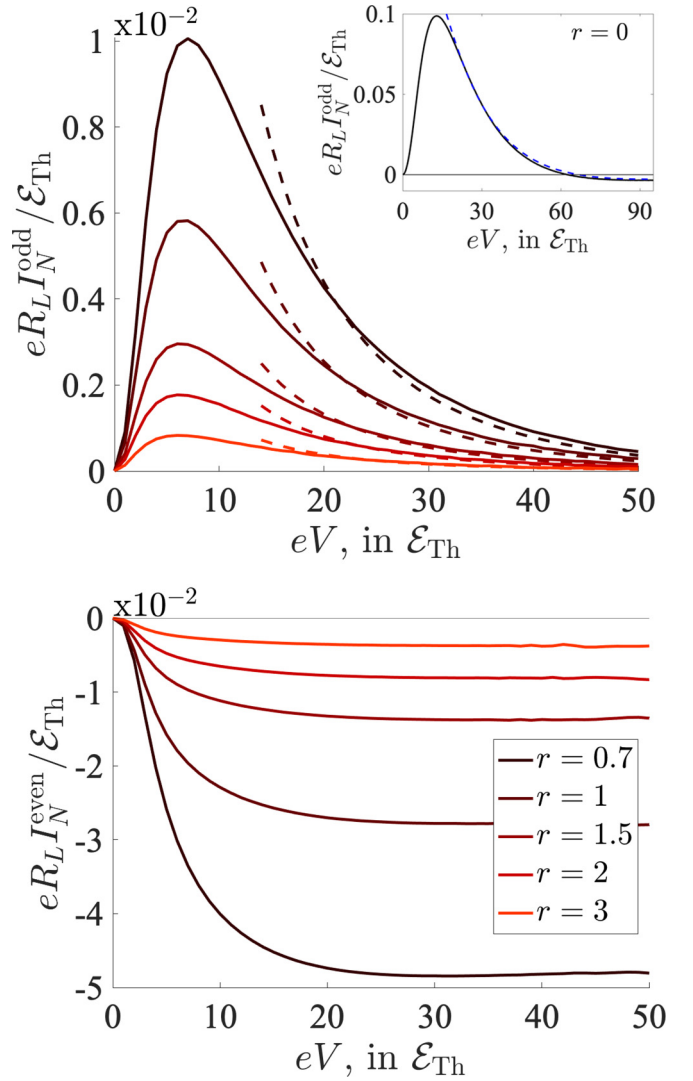

FIG. 4. Top: The amplitude of the odd-in-ϕ oscillations of the current I_N as a function of V at $T \mapsto 0$ for different values of r. The parameter values are the same as in Fig. 2, except $\Delta = 250\mathcal{E}_{\text{Th}}$. Solid lines represent full numerical solution of the Usadel equation (2), dashed lines correspond to the analytical result, cf. Eq. (51). The latter equation provides a good approximation starting from $eV \gtrsim 20\mathcal{E}_{\text{Th}}$ down to the lowest values of r employed in our calculation. Inset: The same quantity evaluated in the limit of fully transparent interfaces and $\Delta = 100\mathcal{E}_{\text{Th}}$. Dashed line corresponds to Eq. (B4). Bottom: Amplitude of the even-in-ϕ oscillations of I_N.

between 0 and π states depending on the applied voltage bias. In contrast, nonvanishing Aharonov-Bohm-like currents do survive in asymmetric structures. The physics of such devices is dominated by a tradeoff between Josephson and Aharonov-Bohm-like quantum coherent contributions to the current I_S, leading to the (I_0, ϕ_0)-junction state at sufficiently high bias voltages [37,38]. Hence, the current-phase relation $I_S(\phi)$ can be manipulated by external voltage bias, temperature, and topology of the setup.

The current $I_N(\phi)$ flowing in the normal contour is also 2π-periodic function of the superconducting phase difference ϕ, i.e., it is directly affected by the proximity induced long-range quantum coherence. With the aid of our symmetry arguments

we demonstrated that in symmetric Andreev interferometers, the current $I_N(\phi, V)$ is an even function of ϕ associated with the Aharonov-Bohm-like contribution.

A nontrivial effect discovered here is that in asymmetric crosslike interferometers the current I_N develops an odd harmonics I_N^{odd}, cf. Eq. (50). The appearance of this contribution is particularly interesting because it can be attributed neither to the Aharonov-Bohm effect nor to the Josephson physics. In fact, our analysis demonstrates that the origin of the term I_N^{odd} is linked to violation of yet one more (electron-hole) symmetry that occurs under nonzero phase bias due to sequential Andreev reflections at different NS interfaces [39]. In the tunneling limit the magnitude of this effect is controlled by $\sin\phi$ thereby resulting in a Josephson-like contribution $I_N^{\text{odd}} \propto \sin\phi$ to the current $I_N(\phi, V)$ between normal terminals. Similarly to $I_S(\phi)$, the current-phase relation $I_N(\phi)$ can also be manipulated by external voltage bias, temperature and topology of the interferometer.

Finally, we note that electron-hole symmetry violation is believed to also be responsible for large thermoelectric effects in Andreev interferometers [39,44]. Our work, therefore, establishes an intimate relation between the current I_N and thermoelectricity in hybrid superconducting nanostructures [45].

To conclude, we developed a detailed theory of quantum coherent charge transport in phase-and-voltage-biased asymmetric crosslike Andreev interferometers. The electron currents in both superconducting and normal contours demonstrate the presence of both even and odd 2π periodic in ϕ contributions. We identified key physical mechanisms responsible for different contributions to these currents, and described their nontrivial behavior depending on the applied voltage, temperature, and the system topology. Our findings allow for full control of the current pattern in biased Andreev interferometers, thus rendering them particularly promising for future applications in modern electronics.

APPENDIX A: SYMMETRIC ANDREEV INTERFEROMETERS

Let us focus our attention on the two special cases: (i) symmetric connectors to S terminals with $l_{S1} = l_{S2}$ and $r_L = r_R$ and (ii) symmetric connectors to N terminals with $l_{N1} = l_{N2}$.

In the case (i), we observe an extra symmetry related to the possibility of interchanging the terminals $S_1 \leftrightarrow S_2$ with simultaneous inversion of the phase $\phi \to -\phi$ implying that all the functions $V_1(\phi, V)$, $V_2(\phi, V)$, $I_{N1}(\phi, V_1, V_2)$, $I_{N2}(\phi, V_1, V_2)$ are even in ϕ, cf. Eq. (24). Besides that,

we have

$$I_{S1}(\phi, V) = -I_{S2}(-\phi, V), \qquad \text{(A1)}$$

$$I_{S2}(\phi, V) = -I_{S1}(-\phi, V). \qquad \text{(A2)}$$

Combining these equations with Eq. (22) we arrive at the relation (23).

In the case (ii), our system is symmetric with respect to interchanging the normal terminals $N_1 \leftrightarrow N_2$. Then we have

$$I_{S1}(\phi, V_2, V_1) = I_{S1}(\phi, V_1, V_2), \qquad \text{(A3)}$$

$$I_{S2}(\phi, V_2, V_1) = I_{S2}(\phi, V_1, V_2), \qquad \text{(A4)}$$

$$I_{N1}(\phi, V_2, V_1) = -I_{N2}(\phi, V_1, V_2), \qquad \text{(A5)}$$

$$I_{N2}(\phi, V_2, V_1) = -I_{N1}(\phi, V_1, V_2). \qquad \text{(A6)}$$

Let us define $\delta V = V_1 + V/2 = V_2 - V/2$. By symmetry in the case (ii) the function δV is even in V. It follows from Eq. (19) that for $\phi \to -\phi$, $V \to -V$ we get

$$
\begin{aligned}
&I_{S1}(\phi, -V/2 + \delta V(\phi), V/2 + \delta V(\phi)) \\
&= -I_{S1}(-\phi, -(-V/2 + \delta V(\phi)), -(V/2 + \delta V(\phi)) \\
&= -I_{S1}(-\phi, -V/2 - \delta V(\phi), V/2 - \delta V(\phi)). \quad \text{(A7)}
\end{aligned}
$$

Here we also employed Eq. (A3). Note that the currents I_{S1}, I_{S2} are even functions of V and, hence, we obtain

$$\delta V(\phi, V) = -\delta V(-\phi, V), \qquad \text{(A8)}$$

i.e., δV turns out to be an odd function of the superconducting phase ϕ.

Applying the relations (A3), (A8) and (19) to the current I_{S1} we get

$$
\begin{aligned}
I_{S1}(\phi, V_1(\phi), V_2(\phi)) &= -I_{S1}(-\phi, -V_2(\phi), -V_1(\phi)) \\
&= -I_{S1}(-\phi, V_1(-\phi), V_2(-\phi)), \quad \text{(A9)}
\end{aligned}
$$

implying that the current I_S again turns out to be an odd function of the phase ϕ, i.e. just like in the case (i) it obeys the relation (23).

Furthermore, making use of the relations (21), (A5), (A6), and (A8) we recover the following properties of the current I_{N1}:

$$
\begin{aligned}
I_{N1}(\phi, V_1(\phi), V_2(\phi)) &= -I_{N2}(-\phi, -V_1(\phi), -V_2(\phi)) \\
&= I_{N1}(-\phi, -V_2(\phi), -V_1(\phi)) \\
&= I_{N1}(-\phi, V_1(-\phi), V_2(-\phi)), \quad \text{(A10)}
\end{aligned}
$$

implying that the current I_N obeys the relation (24), thus being an even function of the phase ϕ.

Obviously, the relations (23) and (24) are also obeyed in a special case of fully symmetric Andreev interferometers with $l_{S1} = l_{S2}$, $r_L = r_R$, and $l_{N1} = l_{N2}$. In this case we have $V_2 = -V_1 = V/2$, i.e., the potentials V_1 and V_2 do not depend on ϕ.

APPENDIX B: TRANSPARENT SN INTERFACES

While the main part of our paper is devoted to the tunneling limit described by KL boundary conditions (15), it is useful

to extend our analysis to the case of fully transparent SN interfaces corresponding to the limit $r = 0$. In particular, we performed a numerical analysis of the current I_N (the current I_S was investigated in Refs. [37,38]). The corresponding results are displayed in Fig. 4 at different values of r, including $r = 0$ in the inset of Fig. 4.

In the case of fully transparent SN interfaces and in the limit of high voltages $\mathcal{E}_{\text{Th}} \ll e|V_{1,2}| < \Delta$ one can also derive an explicit expression for the odd harmonic of the current

I_N. Employing the approach developed in Ref. [38] one can easily find the anomalous Green's function in the normal wires connected to the normal terminals. We obtain

$$F^R = F_c^R e^{i\lambda x}, \quad \tilde{F}^R = \tilde{F}_c^R e^{i\lambda x}, \tag{B1}$$

where x is the distance from the crossing point, and F_c^R is the anomalous Green's function evaluated at this crossing point

$$F_c = -\frac{8i\mathcal{A}_{S1}f_S e^{i\lambda l_{S1}} e^{i\phi_L}}{\mathcal{A}_{S1} + \mathcal{A}_{S2} + \mathcal{A}_{N1} + \mathcal{A}_{N2}} - \frac{8i\mathcal{A}_{S2}f_S e^{i\lambda l_{S2}} e^{i\phi_R}}{\mathcal{A}_{S1} + \mathcal{A}_{S2} + \mathcal{A}_{N1} + \mathcal{A}_{N2}}. \tag{B2}$$

Here we defined

$$f_S(\epsilon) = \tan\left[\frac{1}{4}\arcsin\frac{|\Delta|}{\sqrt{|\Delta|^2 - \epsilon^2}}\right]. \tag{B3}$$

The function $\tilde{F}_c$ can be recovered from Eq. (B2) by replacing F_c by $-\tilde{F}_c$ and $\phi_{L,R}$ by $-\phi_{L,R}$. Then it is straightforward to derive the function $\mathcal{Y}$ and evaluate the integral in Eq. (50). In the case of equal cross sections we obtain

$$\frac{eR_L I_N^{\text{odd}}}{\mathcal{E}_{\text{Th}}} \approx \frac{4\sin\phi}{l_{N1} + l_{N2}} \frac{L^2}{l_{S1}^2 + l_{S2}^2} \sum_{i=1,2}(-1)^{i+1}f_S^2(e|V_i|)\exp\left(-\sqrt{\frac{e|V_i|}{\mathcal{E}_{\text{Th}}}}\right)$$

$$\times \left[L\sin\left(\frac{l_{S1} - l_{S2}}{L}\sqrt{\frac{e|V_i|}{\mathcal{E}_{\text{Th}}}}\right) + (l_{S1} - l_{S2})\cos\left(\frac{l_{S1} - l_{S2}}{L}\sqrt{\frac{e|V_i|}{\mathcal{E}_{\text{Th}}}}\right)\right]. \tag{B4}$$

As shown in the inset of Fig. 4, this analytic expression perfectly matches with our numerical result at $eV \gtrsim 20\mathcal{E}_{\text{Th}}$.

In addition, Eq. (B4) can be used to estimate the maximum value of the current I_N^{odd}.

[1] W. Belzig, F. K. Wilhelm, C. Bruder, G. Schön, and A. D. Zaikin, Superlatt. Microstruct. **25**, 1251 (1999).

[2] A. Fornieri and F. Giazotto, Nature Nanotech. **12**, 944 (2017).

[3] F. Giazotto, T. T. Heikkilä, A. Luukanen, A. M. Savin, and J. P. Pekola, Rev. Mod. Phys. **78**, 217 (2006).

[4] J. Eom, C.-J. Chien, and V. Chandrasekhar, Phys. Rev. Lett. **81**, 437 (1998).

[5] D. A. Dikin, S. Jung, and V. Chandrasekhar, Phys. Rev. B **65**, 012511 (2001).

[6] A. Parsons, I. A. Sosnin, and V. T. Petrashov, Phys. Rev. B **67**, 140502(R) (2003).

[7] P. Cadden-Zimansky, Z. Jiang, and V. Chandrasekhar, New J. Phys. **9**, 116 (2007).

[8] C. D. Shelly, E. A. Matrozova, and V. T. Petrashov, Sci. Adv. **2**, e1501250 (2016).

[9] A. F. Volkov and A. V. Zaitsev, Phys. Rev. B **53**, 9267 (1996).

[10] A. F. Volkov and H. Takayanagi, Phys. Rev. Lett. **76**, 4026 (1996).

[11] A. F. Volkov and H. Takayanagi, Phys. Rev. B **56**, 11184 (1997).

[12] R. Seviour, C. Lambert, and A. Volkov, J. Phys.: Condens. Matter **10**, L615 (1998).

[13] A. Volkov, R. Seviour, and V. Pavlovskii, Superlatt. Microstruct. **25**, 647 (1999).

[14] A. Brinkman, A. A. Golubov, H. Rogalla, F. K. Wilhelm, and M. Y. Kupriyanov, Phys. Rev. B **68**, 224513 (2003).

[15] A. F. Volkov and V. V. Pavlovsky, JETP Lett. **64**, 670 (1997).

[16] T. H. Stoof and Y. V. Nazarov, Phys. Rev. B **54**, R772 (1996).

[17] A. A. Golubov, F. K. Wilhelm, and A. D. Zaikin, Phys. Rev. B **55**, 1123 (1997).

[18] H. Nakano and H. Takayanagi, Solid State Commun. **80**, 997 (1991).

[19] V. T. Petrashov, V. N. Antonov, P. Delsing, and T. Claeson, Phys. Rev. Lett. **74**, 5268 (1995).

[20] H. Courtois, P. Gandit, D. Mailly, and B. Pannetier, Phys. Rev. Lett. **76**, 130 (1996).

[21] J. M. Byers and M. E. Flatté, Phys. Rev. Lett. **74**, 306 (1995).

[22] G. Deutscher and D. Feinberg, Appl. Phys. Lett. **76**, 487 (2000).

[23] D. Beckmann, H. B. Weber, and H. v. Löhneysen, Phys. Rev. Lett. **93**, 197003 (2004).

[24] S. Russo, M. Kroug, T. M. Klapwijk, and A. F. Morpurgo, Phys. Rev. Lett. **95**, 027002 (2005).

[25] P. Cadden-Zimansky and V. Chandrasekhar, Phys. Rev. Lett. **97**, 237003 (2006).

[26] D. S. Golubev and A. D. Zaikin, Phys. Rev. B **76**, 184510 (2007).

[27] M. S. Kalenkov and A. D. Zaikin, Phys. Rev. B **76**, 224506 (2007).

[28] D. S. Golubev, M. S. Kalenkov, and A. D. Zaikin, Phys. Rev. Lett. **103**, 067006 (2009).

[29] A. Brinkman and A. A. Golubov, Phys. Rev. B **74**, 214512 (2006).

[30] A. D. Zaikin and G. F. Zharkov, Fiz. Nizk. Temp. **7**, 375 (1981) [Sov. J. Low Temp. Phys. **7**, 181 (1981)].

[31] P. Dubos, H. Courtois, B. Pannetier, F. K. Wilhelm, A. D. Zaikin, and G. Schön, Phys. Rev. B **63**, 064502 (2001).

[32] A. A. Golubov, M. Y. Kupriyanov, and E. Il'Ichev, Rev. Mod. Phys. **76**, 411 (2004).

[33] A. F. Volkov, Phys. Rev. Lett. **74**, 4730 (1995).

[34] F. K. Wilhelm, G. Schön, and A. D. Zaikin, Phys. Rev. Lett. **81**, 1682 (1998).

[35] S.-K. Yip, Phys. Rev. B **58**, 5803 (1998).

[36] J. J. A. Baselmans, A. F. Morpurgo, B. J. Van Wees, and T. M. Klapwijk, Nature (London) **397**, 43 (1999).

[37] P. E. Dolgirev, M. S. Kalenkov, and A. D. Zaikin, Phys. Rev. B **97**, 054521 (2018).

[38] P. E. Dolgirev, M. S. Kalenkov, and A. D. Zaikin, Sci. Rep. **9**, 1301 (2019).

[39] M. S. Kalenkov and A. D. Zaikin, Phys. Rev. B **95**, 024518 (2017).

[40] N. Schopohl and K. Maki, Phys. Rev. B **52**, 490 (1995).

[41] N. Schopohl, arXiv:cond-mat/9804064.

[42] M. Y. Kuprianov and V. F. Lukichev, Zh. Eksp. Teor. Fiz. **94**, 149 (1988).

[43] Taking advantage of the normalization condition $\check{G}^2 = \check{1}$ it becomes possible to derive the expression for I_N to the first order in $1/r^2$ without expanding the spectral functions γ, $\tilde{\gamma}$ to the next order.

[44] P. E. Dolgirev, M. S. Kalenkov, and A. D. Zaikin, Phys. Status Solidi (RRL) **13**, 1800252 (2019).

[45] M. S. Kalenkov, P. E. Dolgirev, and A. D. Zaikin (unpublished).